High-order I-stable centered difference schemes for viscous compressible flows

Weizhu Bao *
Department of Computational Science
National University of Singapore, Singapore 117543
Shi Jin †
Department of Mathematical Science, Tsinghua University,
Beijing 100084, China and Department of Mathematics
University of Wisconsin-Madison, Madison 53706, USA.

Dedicated to Professor Yu-Lin Zhou on the occasion of his 80th birthday

Abstract

In this paper we present high-order I-stable centered difference schemes for the numerical simulation of viscous compressible flows. Here I-stability refers to time discretizations whose linear stability regions contain part of the imaginary axis. This class of schemes has a numerical stability independent of the cell-Reynolds number Rc, thus allows one to simulate high Reynolds number flows with relatively larger Rc, or coarser grids for a fixed Rc. On the other hand, Rc cannot be arbitrarily large if one tries to obtain adequate numerical resolution of the viscous behavior. We investigate the behavior of high-order I-stable schemes for Burgers' equation and the compressible Navier-Stokes equations. We demonstrate that, for the second order scheme, $Rc \leq 3$ is an appropriate constraint for numerical resolution of the viscous profile, while for the fourth-order schemes the constraint can be relaxed to $Rc \leq 6$. Our study indicates that the fourth order scheme is preferable: better accuracy, higher resolution, and larger cell-Reynolds numbers.

1 Introduction

Compressible flows with high Reynolds numbers, or, more generally, systems of conservation laws with small viscosities, remain a challenging numerical problem, even with great progress in the development of modern shock capturing methods for inviscid flows (the Euler equations) or systems of conservation laws in the last two decades. On the one hand, due to the constraint on the computing capacity, one attempts to simulate high Reynolds number flow with relative coarse grids (larger cell-Reynolds numbers), but on the other hand, when the cell-Reynolds number becomes too large, one loses appropriate resolution on the viscous effect and the numerical solutions become unphysical.

*Email address: bao@cz3.nus.edu.sg. Research supported by the National University of Singapore grant No. R-151-000-016-112.

†Email address: jin@math.wisc.edu. Research supported in part by NSF grant No. DMS-9704957 and DMS-0196106.

Due to the great success of modern shock capturing methods for hyperbolic systems, a very natural idea for the simulation of the viscous flows seems to be the application of a shock capturing method for the convection terms, coupled with some centered differences for the viscosity term. By building a numerical viscosity into the scheme which reduces the accuracy to first order across the discontinuities in order to suppress the numerical oscillations, shock capturing schemes are very effective in simulating inviscid flows and hyperbolic systems of conservation laws [13]. Since the main idea of shock-capturing is underresolution across the discontinuity, when simulating a slightly viscous flows where viscous effect is important, the mixture of numerical viscosities with the physical ones become a subtle issue.

In this paper, we seek an alternative approach by using simply high order centered difference schemes. This approach allows zero numerical viscosity, thus guarantees that, under enough resolution, the viscous effect observed numerically is purely physical. However, the traditional second order centered difference schemes for slightly viscous convection equations has a cell-Reynolds number constraint $Rc \leq 2$. To break this stability barrier, we take the method of line approach and use the so-called I-stable time discretization, which yields a numerical stability independent of Rc.

We call that a time-discretization for an ordinary differential equation is **I-stable** if the linear stability region contains part of the imaginary axis. In [19] Vichnevetsky studied the stability charts in the numerical approximation of partial differential equations. He first found that the linear stability regions of some time-discretization schemes contain part of the imaginary axis and applied these schemes to linear hyperbolic and advection-diffusion equations. In [3, 4], E and Liu realized that to solve the incompressible Navier-Stokes equations, using the fourth-order Runge-Kutta method (which is I-stable according to the above definition) along with a fourth-order centered difference for the convection removes the cell-Reynolds number constraint, thus allows them to simulate incompressible flows with very high Reynolds numbers. Choi and Liu [2] introduced a class of three-stage, second order Runge-Kutta method (which is I-stable) for the compressible Euler equations, and observed good convergence property toward the steady-state solution. This is the scheme we will explore here.

While the I-stable scheme has a remarkable stability property, which allows one to use an arbitrarily large cell-Reynolds number, in practice, this can never be done if one wants to resolve the viscous effect. Failing to resolve adequately the viscous effect will simply produce the results for the inviscid equations, rather than the viscous equations. The rule of the game is to use relatively larger cell-Reynolds number (if stability allows) but still resolve the viscous effect without numerical oscillations. It is the goal of this paper to investigate the suitable cell-Reynolds number constraint for viscous conservation laws using high-order I-stable centered differences. We use the Burgers' equation and the compressible Navier-Stokes equations as examples to study this issue.

We observe that, when using a second-order I-stable centered difference scheme, $Rc \leq 3$ is an appropriate constraint, while for the forth-order I-stable schemes this can be relaxed to $Rc \leq 6$. Within this range of Rc the numerical schemes are stable and are essentially non-oscillatory. This significantly improves the traditional cell-Reynolds number constraint $Rc \leq 2$, and sheds light on a promising direction to develop numerical schemes for compressible flows with high Reynolds numbers.

This paper is organized as follows: In the next section, we introduce the high-order

I-stable centered difference for viscous conservation laws. In section 3, using the Burgers' equation as an example, we investigate the effect of the cell-Reynolds number for different time and spatial discretizations. In section 4, we propose the fourth-order I-stable scheme for the 2-D compressible Navier-Stokes equations. We study numerically the effect of cell-Reynolds number using flows in a driven cavity and a Buoying-driven cavity. We end in section 5 with some discussions.

2 For systems of conservation laws with small viscosity

Consider the scalar conservation laws with viscosity:

$$\partial_t u + \partial_x f(u) = \nu \partial_{xx} u \,. \tag{2.1}$$

Let $c = \sup |f'(u)|$ be the supreme of the characteristic speed, h be the grid size, and u_j be the numerical approximation of $u(x_j)$. The cell Reynolds number is defined as: $Rc = ch/\nu$

We use the method of line approach to solve (2.1), which decouples the spatial discretization from the time discretization. We consider the second order centered difference

$$\partial_t u_i + \frac{1}{2h}\left[f(u_{i+1}) - f(u_{i-1})\right] = \frac{\nu}{h^2}(u_{i+1} - 2u_i + u_{i-1}), \tag{2.2}$$

and the fourth-order centered difference

$$\begin{aligned} &\partial_t u_i + \frac{1}{12h}\left[f(u_{j-2}) - 8f(u_{j-1}) + 8f(u_{j+1}) - f(u_{j+2})\right] \\ &= \frac{\nu}{12h^2}\left(-u_{j-2} + 16u_{j-1} - 30u_j + 16u_{j+1} - u_{j+2}\right). \end{aligned} \tag{2.3}$$

The discrete systems (2.2) or (2.3) can be written as a system of ordinary differential equations (ODEs)

$$\frac{dU}{dt} = F(U), \tag{2.4}$$

where $U = U(t)$ is a vector function of t and F is a vector function of U and t. Let Δt be the time step. Consider the following four explicit time discretizations for the ODE system (2.4):

1. Forward Euler (FE)

$$U^{k+1} = U^k + \triangle t F(U^k); \tag{2.5}$$

2. Classical second-order Runge-Kutta (RK2)

$$U^{k+1} = U^k + \triangle t K_2, \qquad K_1 = F(U^k)\,, \quad K_2 = F\left(U^k + \triangle t\, K_1/2\right)\,. \tag{2.6}$$

3. Second-order three-stage Runge-Kutta (RK2*)

$$\begin{aligned} U^{k+1} &= U^k + \triangle t K_3, \\ K_1 &= F(U^k)\,, \quad K_2 = F\left(U^k + \triangle t\, K_1/3\right)\,, \quad K_3 = F\left(U^k + \triangle t\, K_2/2\right)\,. \end{aligned} \tag{2.7}$$

4. Fourth-order Runge-Kutta (RK4)

$$\begin{aligned} U^{k+1} &= U^k + \frac{\triangle t}{6}(K_1 + 2K_2 + 2K_3 + K_4), \qquad K_1 = F(U^k)\,, \\ K_2 &= F\left(U^k + \triangle t\, K_1/2\right), \quad K_3 = F\left(U^k + \triangle t\, K_2/2\right), \quad K_4 = F(U^k + \triangle t K_3). \end{aligned} \tag{2.8}$$

When $\nu = 0$, the Forward Euler method in time coupled with a centered difference in space is notoriously linearly unconditionally unstable [17]. With $\nu > 0$, the Euler method in time with centered difference (2.2) in space has the stability constraint $Rc \leq 2$, in additional to the usual CFL condition $\nu \Delta t/h^2 \leq 1/2$ [17, 5]. This imposes a restriction for the grid size for any given ν, thus limits the Reynolds number for any given grid size, an unattractive fact for the simulation of conservation laws with small viscosity or fluid flows with high Reynolds numbers. One observes similar behavior for the second order classical Runge-Kutta method (RK2).

However, past experience [3, 4] shows that, by replacing the FE or RK2 in time by classical Runge-Kutta method of order at least three, or the modified three-stage, second order Runge-Kutta method (RK2*), this stability constraint is lifted. Still lack of rigorous theory, nevertheless, a linear stability analysis provides a clue to this phenomenon [5].

In fact, the usual stability analysis for numerical methods for ODEs deals with the following prototype linear scalar problem:

$$v' = \lambda v. \tag{2.9}$$

Applying (FE) to this linear equation (2.9) gives

$$v^{k+1} = (1 + \lambda \Delta t)v^k = (1 + z)v^k, \tag{2.10}$$

where $z = \lambda \Delta t$. Then the region of absolute stability is given by

$$|1 + z| \leq 1. \tag{2.11}$$

Similarly, the regions of absolute stability for RK2, RK2* and RK4 are given by:

$$\text{For RK2}: \quad \left|1 + z + \frac{1}{2!}z^2\right| \leq 1; \tag{2.12}$$

$$\text{For RK2}^*: \quad \left|1 + z + \frac{1}{2!}z^2 + \frac{1}{3!}z^3\right| \leq 1; \tag{2.13}$$

$$\text{For RK4}: \quad \left|1 + z + \frac{1}{2!}z^2 + \frac{1}{3!}z^3 + \frac{1}{4!}z^4\right| \leq 1. \tag{2.14}$$

In Figure 1, we draw the regions of absolute stability for the ODE solvers FE, RK2, RK2* and RK4. From the figure, one can see that the regions of absolute stability of FE and RK2 do not cover any interval along the imaginary axis. On the other hand, the regions of absolute stability of RK2* and RK4 cover $i\left[-\sqrt{3}, \sqrt{3}\right]$ and $i[-2.85, 2.85]$ along the imaginary axis, respectively.

Let us return back to the PDE (2.1) with the linear flux $f(u) = au$, i.e.,

$$\partial_t u + a\partial_x u = \nu \partial_{xx} u\,. \tag{2.15}$$

Assuming a periodic boundary condition $u(t, 0) = u(t, 2\pi)$, the solution can be expanded in a Fourier series, $u(x, t) = \sum_k \tilde{u}_k(t) \exp(ikx)$. For each mode $\tilde{u}_k(t)$ we have

$$\partial_t \tilde{u}_k(t) = (-iak - \nu k^2)\tilde{u}_k(t) := \lambda \tilde{u}_k(t), \tag{2.16}$$

with $\lambda = -iak - \nu k^2$. When $\nu = 0$, λ lies on the imaginary axis, while when $\nu > 0$ but small, λ is on the left-half of the plane, but very close to the imaginary axis. Similar

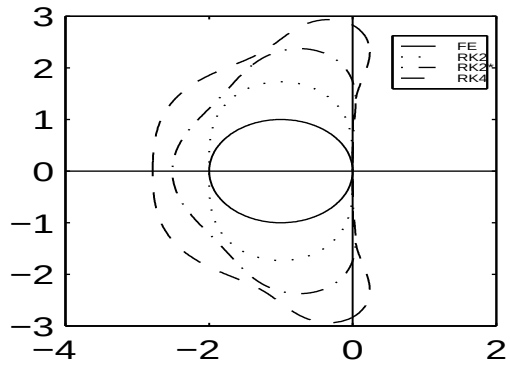

Figure 1: Regions of absolute stability for ODE solvers FE, RK2, RK2* and RK4

eigenvalue behavior occurs for the discrete systems (2.2) and (2.3). Expand the solution of (2.2) or (2.3) with $f(u) = au$ using a discrete Fourier series $u_i(t) = \sum_{k=0}^{n} \tilde{u}_k(t) \exp(ikx_j)$. For each mode k of the solution of (2.2), we have

$$\partial_t \tilde{u}_k(t) = \left(-i\frac{a}{h}\sin(kh) - 4\frac{\nu}{h^2}\sin^2(kh/2) \right) \tilde{u}_k(t) := \lambda \tilde{u}_k(t). \tag{2.17}$$

Similarly, for each mode k of the solution of (2.3), we have

$$\begin{aligned} \partial_t \tilde{u}_k(t) &= \left(-i\frac{a}{6h}(8\sin(kh) - \sin(2kh)) - \frac{\nu}{3h^2}(16\sin^2(kh/2) - \sin^2(kh)) \right) \tilde{u}_k(t) \\ &:= \lambda \tilde{u}_k(t). \end{aligned} \tag{2.18}$$

The above analysis reveals that both RK2* and RK4 are I-stable, while FE and RK2 are not. Combining the eigenvalue analysis on the PDE and the stability analysis on the ODE solver, one sees that an I-stable time discretization is stable for centered differences with a suitable time-step, but imposes no constraint on Rc, even with $\nu = 0$ (so theoretically Rc can be infinite!).

We would like to point out that the classical Lax-Wendroff scheme [10] and the MacCormack scheme [14] also possess a stability independent of Rc, provided a suitable CFL condition is satisfied. This is easy to understand since both are stable for the inviscid equation ($\nu = 0$), and the viscosity term only enhances their stability property. However, the higher order extension of the Lax-Wendroff idea requires numerical evaluation of not only the Jacobi matrix of the flux, but also Hessian matrix and the third order derivative of $f(u)$, while for the MacCormack scheme, based on the predictor-corrector idea, is not easy to extend to higher order. The approach using method of line, nevertheless, can be extended to any order of accuracy. Another way to enhance numerical stability is to add artificial numerical viscosity, see for example [18, 16]. However, this approach, like other shock capturing methods, deviates from our purpose here since we try to avoid any numerical viscosity. Traveling wave schemes introduced in [7] seem to improve the Rc but they lack the generality to be applied to complicated physical systems.

For systems of conservation laws with viscosity, the above approach applies **componentwise** to the system, with similar stability property.

For problems with small parameter, such as the viscosity coefficient, the stability is not the only issue of concern. Although theoretically the Rc can be arbitrary for I-stable schemes, if one fails to resolve the small parameter numerically to a certain degree, one may miss the viscous effect. Thus a numerical computation for problems with small parameters should balance the issue of **accuracy** and **resolution**, namely, on the one hand, one hopes to use large Rc, but on the other hand, Rc should be suitably small in order to numerically resolve the small viscous effect. See [11] and [15] for a rather general discussion about the resolution power of some high-order finite difference approximations of spatial derivatives.

Below, we investigate these numerical issues for second order ((2.2)+RK2*) and fourth-order ((2.3) + RK4) I-stable centered difference schemes for the Burger's equation and the compressible Navier-Stokes equations. Our experience indicates that the fourth order scheme always achieves better accuracy and higher resolution even with a coarse grid, thus allowing the use of larger Rc. These great advantages greatly compensate the additional cost of the higher order scheme.

3 Burgers' equation

In this section we use Burgers' equation as an example to test the performance of the I-stable schemes introduced in the previous section. The initial-boundary value problem has exact solution, which allows us to carry out a detailed comparison between the numerical solutions and the exact one.

3.1. The analytic problem

Consider the Burgers' equation in conservative form:

$$u_t + \left(u^2/2\right)_x = \nu u_{xx}, \qquad a < x < b, \quad t > 0. \tag{3.1}$$

with initial condition

$$u(x,0) = u_r + 0.5(u_l - u_r)\left[1 - \tanh\left((u_l - u_r)(x - 0.25)/4\nu\right)\right], \qquad a \le x \le b, \tag{3.2}$$

and boundary conditions

$$u(a,t) = u_r + 0.5(u_l - u_r)\left[1 - \tanh\left((u_l - u_r)(a - 0.25 - st)/4\nu\right)\right], \qquad t \ge 0, \tag{3.3}$$

$$u(b,t) = u_r + 0.5(u_l - u_r)\left[1 - \tanh\left((u_l - u_r)(b - 0.25 - st)/4\nu\right)\right], \qquad t \ge 0\,, \tag{3.4}$$

where $s = (u_l + u_r)/2$. The problem (3.1)-(3.4) has the exact solution [13]

$$u^\nu(x,t) = u_r + 0.5(u_l - u_r)\left[1 - \tanh\left((u_l - u_r)(x - 0.25 - st)/4\nu\right)\right]. \tag{3.5}$$

3.2 Discretization

Let $h = (b-a)/n$ denote the grid size, $u_j = u_j(t) \sim u(x_j,t)$, $x_j = a + jh$, for $j = 0, 1, \cdots, n$. The second-order centered discretization (2.2) of (3.1) is

$$\frac{du_j}{dt} = -\frac{u_{j+1}^2 - u_{j-1}^2}{4h} + \nu\frac{u_{j+1} - 2u_j + u_{j-1}}{h^2}, \qquad 1 \le j \le n-1\,. \tag{3.6}$$

The fourth-order centered difference (2.3) of (3.1) gives

$$\begin{aligned}\frac{du_j}{dt} &= -\frac{u_{j-2}^2 - 8u_{j-1}^2 + 8u_{j+1}^2 - u_{j+2}^2}{24h} \\ &\quad +\nu\frac{-u_{j-2} + 16u_{j-1} - 30u_j + 16u_{j+1} - u_{j+2}}{12h^2}, \qquad 1 \le j \le n-1\,. \end{aligned} \tag{3.7}$$

For the fourth-order scheme, we use two "ghost points" u_{-1} and u_{n+1}. The "ghost points" approach for boundary conditions in calculating incompressible viscous flows is widely used and gives promising results [4, 5]. They are calculated by a fourth-order interpolation formula obtained by Taylor expansion:

$$u_{-1} = 5u_0 - 10u_1 + 10u_2 - 5u_3 + u_4, \tag{3.8}$$

$$u_{n+1} = 5u_n - 10u_{n-1} + 10u_{n-2} - 5u_{n-3} + u_{n-4}. \tag{3.9}$$

The cell-Reynolds number is

$$Rc := \frac{h \max|u|}{\nu}\,. \tag{3.10}$$

In next section, we solve the above problem using two I-stable centered schemes, (D2): the second order ((2.2)+RK2*) scheme, and (D4): the fourth-order ((2.3) + RK4) scheme.

3.3. Numerical results

We take $a = 0$, $b = 1$, $u_l = 1.0$ and $u_r = 0.0$. we use the above two schemes to calculate the numerical solutions of the problem (3.1), (3.2), (3.3) and (3.4) for different ν and h. We choose time step $\triangle t$ according to a fixed CFL:= $\frac{\max|u|\triangle t}{h} \equiv 0.5$ in all computations. Table 1 shows the discrete L^1-norm error $\|u^\nu - u_h\|_1 := \sum_{j=0}^n h|u^\nu(x_j, t^n) - u_h^n| = \sum_{j=0}^n \frac{b-a}{n}|u^\nu(x_j, t^n) - u_h^n|$ at $t_n = 1.0$ for different ν and Rc when using the discretization (D2). Table 2 shows the similar results for the discretization (D4). Furthermore Figure 2 shows the numerical solution for $\nu = 0.000625$ and different Rc at $t = 1$.

$\|u^\nu - u_h\|_1$	$Rc = 1$	$Rc = 2$	$Rc = 3$	$Rc = 4$	$Rc = 8$
$\nu = 0.01$	5.21E-4	2.16E-3	4.99E-3	1.01E-2	
$\nu = 0.005$	2.60E-4	1.03E-3	2.29E-3	4.42E-3	2.03E-2
$\nu = 0.0025$	1.30E-4	5.14E-4	1.23E-3	2.51E-3	1.29E-2
$\nu = 0.00125$	6.51E-5	2.57E-4	5.76E-4	1.25E-3	5.36E-3
$\nu = 0.000625$	3.25E-5	1.28E-4	3.05E-4	6.27E-4	2.68E-3

Table 1: The discrete L^1 error for (D2) at $t = 1$

From Tables 1-2, one can see that:

1) For fixed Rc, the error is basically the same for different ν. For fixed ν, the error increased quadratically with Rc.

2) To achieve the same accuracy, the (D4) can use Rc twice as big as (D2).

Note the solution has a sharp viscous layer, which prevents both schemes to achieve the desired accuracy for a smooth solution. In this case, the accuracy may not be the best indicator of the performance of a numerical scheme, and the resolution is more appropriate measure. Although one cannot quantify the resolution, Figure 2 indicates that

$\|u^\nu - u_h\|_1$	$Rc = 1$	$Rc = 2$	$Rc = 4$	$Rc = 6$	$Rc = 8$
$\nu = 0.01$	1.53E-4	2.73E-4	2.83E-3	9.52E-3	
$\nu = 0.005$	8.07E-5	1.24E-4	1.58E-3	5.20E-3	1.16E-2
$\nu = 0.0025$	4.93E-5	6.54E-5	6.00E-4	3.11E-3	7.91E-3
$\nu = 0.00125$	4.25E-5	3.99E-5	3.02E-4	1.27E-3	2.59E-3
$\nu = 0.000625$	5.69E-5	3.71E-5	1.56E-4	7.93E-4	1.29E-3

Table 2: The discrete L^1 error for (D4) at $t = 1$

the numerical shock layer matches well with the physical one when $Rc \leq 3$ for (D2) and when $Rc \leq 6$ for (D4).

4 The Compressible Navier-Stokes equations

In this section we consider numerical discretization for the compressible viscous flows. Since our previous numerical tests clearly indicate that the fourth order I-stable scheme outperforms the second order scheme, in this section we only propose the fourth order scheme for the discretization of the compressible Navier-Stokes equations.

4.1 The equations

We consider two-dimensional, dimensionless, compressible Navier-Stokes equations [12, 20]:

$$\frac{\partial \rho}{\partial t} + \frac{\partial \rho u}{\partial x} + \frac{\partial \rho v}{\partial y} = 0, \tag{4.1}$$

$$\frac{\partial \rho u}{\partial t} + \frac{\partial \rho u^2}{\partial x} + \frac{\partial \rho uv}{\partial y} + \frac{1}{\gamma M^2}\frac{\partial \rho T}{\partial x} = \frac{1}{Re}\left(\frac{4}{3}\frac{\partial^2 u}{\partial x^2} + \frac{\partial^2 u}{\partial y^2} + \frac{1}{3}\frac{\partial^2 v}{\partial x \partial y}\right), \tag{4.2}$$

$$\frac{\partial \rho v}{\partial t} + \frac{\partial \rho uv}{\partial x} + \frac{\partial \rho v^2}{\partial y} + \frac{1}{\gamma M^2}\frac{\partial \rho T}{\partial y} = \frac{1}{Re}\left(\frac{1}{3}\frac{\partial^2 u}{\partial x \partial y} + \frac{\partial^2 v}{\partial x^2} + \frac{4}{3}\frac{\partial^2 v}{\partial y^2}\right) - \frac{\rho}{2\varepsilon Fr}, \tag{4.3}$$

$$\begin{aligned}
&\frac{\partial}{\partial t}\left(\frac{1}{\gamma}\rho T + \frac{\rho}{2}(\gamma-1)M^2(u^2+v^2)\right) + \frac{\partial}{\partial x}\left(\rho u T + \frac{\rho u}{2}(\gamma-1)M^2(u^2+v^2)\right) \\
&+\frac{\partial}{\partial y}\left(\rho v T + \frac{\rho v}{2}(\gamma-1)M^2(u^2+v^2)\right) = \Psi + \frac{(\gamma-1)M^2}{Re}\Phi \\
&+\frac{1}{Pe}\left(\frac{\partial^2 T}{\partial x^2} + \frac{\partial^2 T}{\partial y^2}\right) - \frac{(\gamma-1)M^2}{\varepsilon Fr}\rho v;
\end{aligned} \tag{4.4}$$

with

$$\begin{aligned}
\Psi &= \frac{(\gamma-1)M^2}{Re}\left[\frac{4u}{3}\frac{\partial^2 u}{\partial x^2} + u\frac{\partial^2 u}{\partial y^2} + \frac{u}{3}\frac{\partial^2 v}{\partial x \partial y} + \frac{v}{3}\frac{\partial^2 u}{\partial x \partial y} + v\frac{\partial^2 v}{\partial x^2} + \frac{4v}{3}\frac{\partial^2 v}{\partial y^2}\right], \\
\Phi &= 2\left[\left(\frac{\partial u}{\partial x}\right)^2 + \left(\frac{\partial v}{\partial y}\right)^2 + \frac{1}{2}\left(\frac{\partial u}{\partial y} + \frac{\partial v}{\partial x}\right)^2\right] - \frac{2}{3}\left(\frac{\partial u}{\partial x} + \frac{\partial v}{\partial y}\right)^2,
\end{aligned}$$

where M is the Mach number, Fr the Froude number, Ra the Rayleigh number, Pr the Prandtl number, Re the Reynolds number, Pe the Peclet number, α the thermal diffusivity, γ the ratio of specific heats, and ε the temperature difference parameter. Here we use the equation of state

$$p = \rho RT, \tag{4.5}$$

where R is the gas constant.

4.2 Fourth-order spatial discretization

Let $\mathcal{T}_h$ be the rectangular grid of the physical domain and h be the spatial mesh size. Define the following fourth-order centered spatial difference operators:

$$\begin{aligned}
D_x u(x,y) &= \frac{1}{12h}\left[u(x-2h,y) - 8u(x-h,y) + 8u(x+h,y) - u(x+2h,y)\right], && (4.6)\\
D_y u(x,y) &= \frac{1}{12h}\left[u(x,y-2h) - 8u(x,y-h) + 8u(x,y+h) - u(x,y+2h)\right], && (4.7)\\
D_{xx} u(x,y) &= \frac{1}{12h^2}\left[-u(x-2h,y) + 16u(x-h,y) - 30u(x,y)\right.\\
&\quad \left.+16u(x+h,y) - u(x+2h,y)\right], && (4.8)\\
D_{yy} u(x,y) &= \frac{1}{12h^2}\left[-u(x,y-2h) + 16u(x,y-h) - 30u(x,y)\right.\\
&\quad \left.+16u(x,y+h) - u(x,y+2h)\right] && (4.9)\\
D_{xy} u(x,y) &= \frac{1}{24h^2}\left[10u(x-h,y-h) - 10u(x-h,y+h) - 10u(x+h,y-h)\right.\\
&\quad +10u(x+h,y+h)) - u(x-2h,y-h) + u(x-2h,y+h)\\
&\quad +u(x+2h,y-h) - u(x+2h,y+h) - u(x-h,y-2h)\\
&\quad \left.+u(x-h,y+2h) + u(x+h,y-2h) - u(x+h,y+2h)\right]. && (4.10)
\end{aligned}$$

With these notations, we can then write our forth-order centered difference scheme for the Navier-Stoles equations (4.1)-(4.4) as follows:

$$\frac{d\rho}{dt} + D_x(\rho u) + D_y(\rho v) = 0, \tag{4.11}$$

$$\frac{d(\rho u)}{dt} + D_x(\rho u^2) + D_y(\rho uv) + \frac{D_x(\rho T)}{\gamma M^2} = \frac{1}{Re}\left(\frac{4}{3}D_{xx}u + D_{yy}u + \frac{1}{3}D_{xy}v\right), \tag{4.12}$$

$$\frac{d(\rho v)}{dt} + D_x(\rho uv) + D_y(\rho v^2) + \frac{D_y(\rho T)}{\gamma M^2} = \frac{1}{Re}\left(\frac{1}{3}D_{xy}u + D_{xx}v + \frac{4}{3}D_{yy}v\right) - \frac{\rho}{2\varepsilon Fr}, \tag{4.13}$$

$$\begin{aligned}
&\frac{d}{dt}\left(\frac{1}{\gamma}\rho T + \frac{\rho}{2}(\gamma-1)M^2(u^2+v^2)\right) + D_x\left(\rho uT + \frac{\rho u}{2}(\gamma-1)M^2(u^2+v^2)\right)\\
&+D_y\left(\rho vT + \frac{\rho v}{2}(\gamma-1)M^2(u^2+v^2)\right) = \Psi_h + \frac{(\gamma-1)M^2}{Re}\Phi_h\\
&+\frac{1}{Pe}\left(D_{xx}T + D_{yy}T\right) - \frac{(\gamma-1)M^2}{\varepsilon Fr}\rho v;
\end{aligned} \tag{4.14}$$

with

$$\Psi_h = \frac{(\gamma-1)M^2}{Re}\left[\frac{4u}{3}D_{xx}u + uD_{yy}u + \frac{u}{3}D_{xy}v + \frac{v}{3}D_{xy}u + vD_{xx}v + \frac{4v}{3}D_{yy}v\right], \tag{4.15}$$

$$\Phi_h = 2\left[(D_x u)^2 + (D_y v)^2 + \frac{1}{2}(D_y u + D_x v)^2\right] - \frac{2}{3}(D_x u + D_y v)^2 . \qquad (4.16)$$

The discrete system (4.11)-(4.16) holds at all interior points. Then we apply the forth-order Runge-Kutta scheme (2.8) to discretize the ordinary differential system (4.11)-(4.14).

Boundary conditions are dealt with the "ghost points" approach as follows: For example, suppose $\Gamma = \{(x,0) \ : \ a \le x \le b\}$ is a boundary and the Dirichlet boundary condition or Neumann boundary condition is posed. We always use the "ghost points" $(x_j, -h)$.

1). For the Dirichlet boundary condition $u(x,0) = u_0(x)$, we have that

$$\begin{aligned} u(x_j,0) &= u_0(x_j), & (4.17)\\ u(x_j,-h) &= 5u(x_j,0) - 10u(x_j,h) + 10u(x_j,2h) - 5u(x_j,3h) + u(x_j,4h). & (4.18) \end{aligned}$$

2). For the Neumann boundary condition $\frac{\partial u}{\partial y}(x,0) = g(x)$, we have that

$$\begin{aligned} u(x_j,0) &= \frac{48}{25}u(x_j,h) - \frac{36}{25}u(x_j,2h) + \frac{16}{25}u(x_j,3h) - \frac{3}{25}u(x_j,4h) - \frac{12h}{25}g(x_j), & (4.19)\\ u(x_j,-h) &= \frac{1}{3}\left[-10u(x_j,0) + 18u(x_j,h) - 6u(x_j,2h) + u(x_j,3h)\right] - 4hg(x_j). & (4.20) \end{aligned}$$

The above equations (4.17)-(4.20) are obtained by Taylor expansions and are fourth-order accurate. The boundary conditions at other sides are dealt with in a similar way.

In the next subsection, we use the above scheme to solve several problems of compressible viscous flows.

4.3 Numerical examples

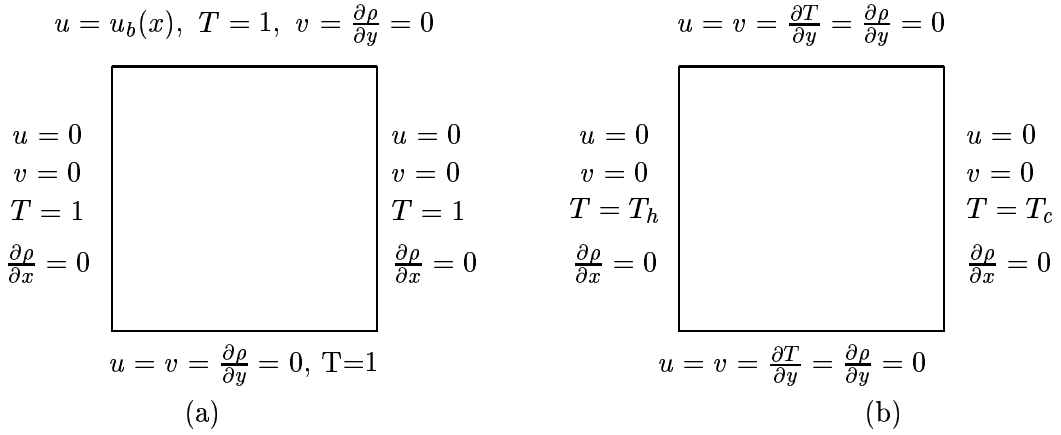

Figure 4. Boundary conditions for: (a). the Lid-driven cavity flow; (b). the buoyancy-driven flow.

Example 4.1. The lid-driven cavity compressible viscous flow

As shown in Figure 4(a), the fluid in the unit square cavity is driven by the moving top at a velocity $u_b(x) = 16x^2(1-x)^2$. This is to avoid the singularity at the two top

corners for velocity in the initial data. We take $M = 0.5$, $\varepsilon = 0.6$, $\gamma = 1.4$, $Fr = 1.0$ and $Pe = 100.0$. In our computation, we take $\triangle t = 0.001$. Figure 3 shows the velocity field and contour of temperature for $Re = 4000$ on a uniform mesh 200×200 (the corresponding $Rc = 20$) at $t = 5.0$.

Example 4.3. The buoyancy-driven cavity compressible viscous flow

The second example is a buoyancy-driven gas flow in a square enclosure [20]. As shown in Figure 4(b), the configuration consists of two insulated horizontal walls and two vertical walls at different temperatures T_h and T_c. In [20], the solution near incompressible regime was presented. We take $M = 0.5$, $\varepsilon = 0.6$, $\gamma = 1.4$, $Fr = 1.0$, $T_h = 0.4$, $T_c = 0.1$ and $Pe = 100.0$. A uniform 100×100 grid is used in our computation. In this computation, we take $\triangle t = 0.0002$. Figure 4 shows the velocity field and contour of temperature for $Re = 600$ at $t = 2.0$. The corresponding cell-Reynolds number is $Rc = 6$. Since the solution becomes discontinuous, when $Rc > 6$, we observed numerical oscillations.

5 Conclusions

In this paper, we propose a high-order centered spatial difference scheme for the numerical simulation of compressible viscous flow. By using I-stable time-discretization methods, the usual cell-Reynolds number constraint $Rc \leq 2$ is greatly relaxed. Under the standard CFL condition, these schemes are stable and with high resolution of the viscous effect when Rc is much greater than 2. Our numerical results show that, for the second-order centered spatial difference scheme coupled with the I-stable second-order three-stage Runge-Kutta time discretization, $Rc \leq 3$ gives quite good resolution for problems involving sharp viscous layers, For the fourth-order centered spatial difference scheme coupled with the classical fourth-order Runge-kutta time discretization, $Rc \leq 6$ gives very good resolution. When applying high-order centered spatial difference schemes, the "ghost points" approach to deal with the boundary condition is recommended and the one-sided high-order spatial difference scheme approach should be avoided or used very carefully. Numerical results also show that the cell-Reynolds number Rc can be chosen much higher when the solution is sufficiently smooth (for example, when the Mach number is very small) than solutions containing large gradients. For applications of the I-stable centered difference schemes for incompressible viscous flows based on a weakly compressible model, we refer to [1].

References

[1] W. Bao and S. Jin, Weakly compressible high-order I-stable central difference schemes for incompressible viscous flows, Comput. Methods Appl. Mech. Engrg., 190(2001) 5009-5026.

[2] H. Choi and J.-G. Liu, The reconstruction of upwind fluxes for conservation laws, its behavior in dynamic and steady state calculations, J. Comput. Phys., 144(1998) 237–256.

[3] W. E and J.-G. Liu, Vorticity boundary condition and related issues for finite difference schemes, J. Comput. Phys., 124(1996), 368-382.

[4] W. E and J.-G. Liu, Essentially compact schemes for unsteady viscous incompressible flows, J. Comput. Phys., 126(1996), 122-138.

[5] W. E and J.-G. Liu, unpublished notes.

[6] U. Ghia, K. N. Ghia and C. T. Shin, High-*Re* solutions for incompressible flow using the Navier-Stokes equations and a multigrid method, J. Comput. Phys., 48(1982), 387-411.

[7] E. Harabetian, A numerical method for viscous perturbation of hyperbolic conservation laws, SIAM J. Num. Anal., 27(1990), 870-884.

[8] S. Hou, Q. Zou, S. Chen, G. Doolen and A. C. Cogley, Simulation of cavity flow by the lattice Boltzmann method, J. Comput. Phys., 118(1995), 329-347.

[9] P. Jorgenson and E. Turkel, Central difference TVD schemes for time dependent and steady state problems, J. Comput. Phys., 107(1993), 297-308.

[10] P.D. Lax and B. Wendroff, Systems of conservation laws, Comm. Pure Appl. Math., 13(1960), 217-237.

[11] S. K. Lele, Compact finite difference schemes with spectral-like resolution, J. Comput. Phys., 103(1992), 16-42.

[12] L. D. Landau and E. M. Lifshitz, Fluid Mechanics, Pergamon Press, Oxford, New York, 1987.

[13] R. J. LeVeque, Numerical Methods for Conservation Laws, rev. ed., Birkhäuser, Basel, 1992.

[14] R. W. MacCormack, The effect of viscosity in hypervelocity impact cratering, AIAA Paper No. 69-354, Cincinati, Ohio, (1969).

[15] K. Mahesh, A family of high order finite difference schemes with good spectral resolution, J. Comput. Phys., 145(1998), 332-358.

[16] R. Peyret and T.D. Taylor, Computational Methods for Fluid Flow, Springer-Verlag, Berlin, 1983.

[17] R. D. Richtmyer and K. W. Morton, Difference Methods for Initial-value Problems, Interscience Publishers, New York, 1967.

[18] B. Sjögreen, High order centered difference Methods for the compressible Navier-Stokes equations, J. Comput. Phys., 117(1995), 67-78.

[19] R. Vichnevtsky, Stability charts in the numerical approximation of partial differential equations: a review, Math. Comput. Simulation, XXI(1979), 170-177.

[20] S. Yu, B. Jiang, N. Liu and J. Wu, The least-squares finite element method for low-Mach-number compressible viscous flows, Int. J. Numer. Methods Engrg., 38(1995), 3591-3610.

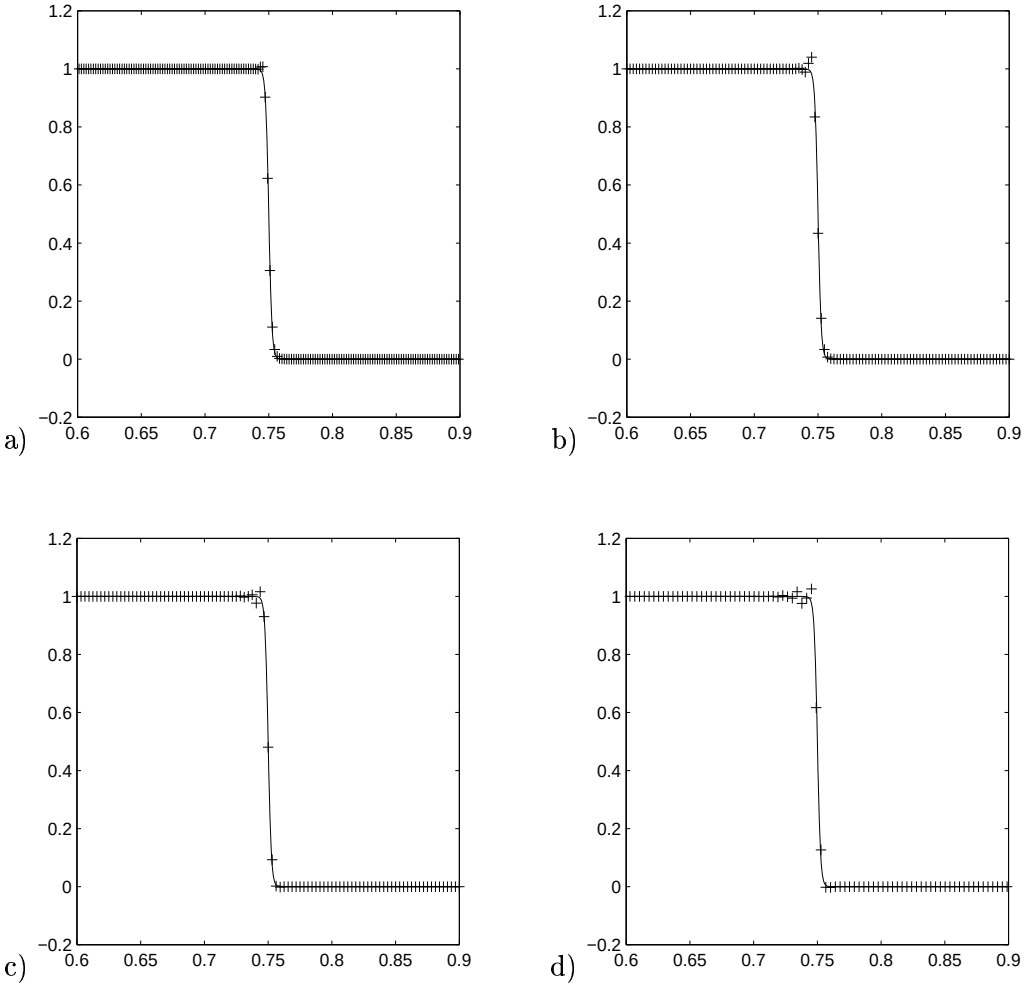

Figure 2. Numerical solutions for $\nu = 0.000625$. Top row: Using the second-order scheme (D2) with a) $Rc = 3$ and b) $Rc = 4$. Bottom row: Using the forth-order scheme (D4) with c) $Rc = 5$ and d) $Rc = 6$.

a) 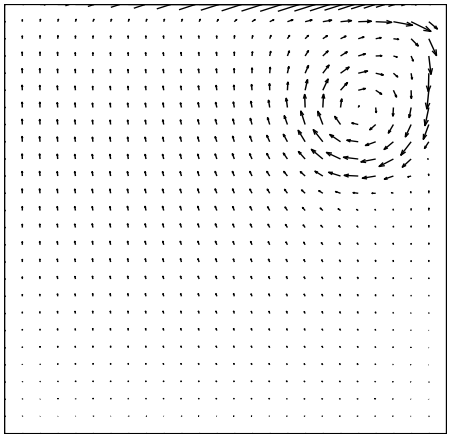 b) 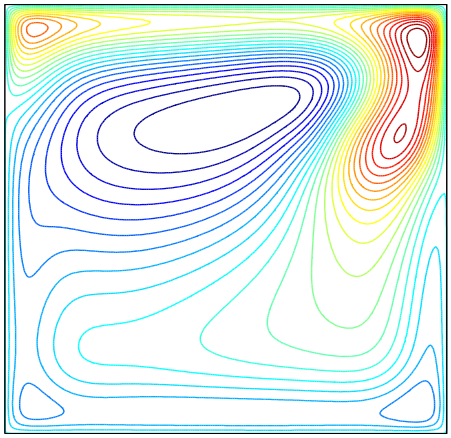

Figure 3 Numerical solutions for the lid-driven cavity flow for $Re = 4000$ on a 200×200 mesh. a) Velocity field, b) Temperature.

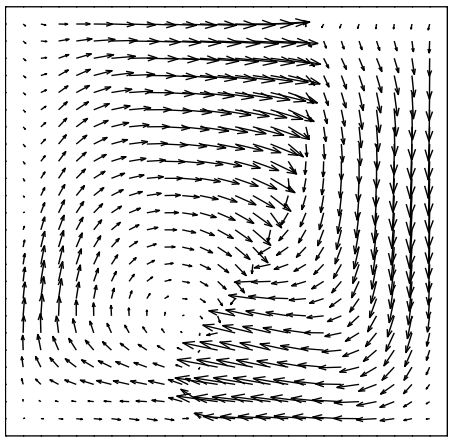 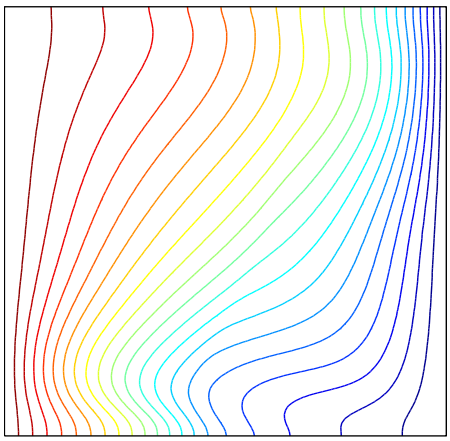

Figure 4 Numerical solutions for the buoyancy-driven cavity flow for $Re = 600$ and $M = 0.5$. a) Velocity field, b) Temperature.